J. Applied Membrane Science & Technology, Vol. 19, December 2016, 19–31

Elimination of an Endocrine Disruptive Chemical by PSf/TiO_2 hybrid Membranes via Membrane Rejection and Photocatalytic Oxidation

V. S. Babu, M. S. Jyothi, Laveena P. D'Souza, R. Shwetharani, Mahesh Padaki*, R. Geetha Balakrishna

Center for Nano and Material Sciences, Jain University, Jakkasandra, Kanakapura Taluk, Ramanagar District–562112, India

ABSTRACT

This study reports removal of oxybenzone from TiO_2 nanoparticles and those incorporated mixed matrix membrane. Polysulfone and TiO_2 nanoparticles mixed matrix membrane were prepared by Diffusion Induced Phase Separation (DIPS) method. The TiO_2 nanoparticles and membranes were characterized by XRD, SEM, TEM, Raman spectroscopy and FESEM techniques; analysis depicts 100% anatase with spherical crystallite size averaging around 17 nm. The mixed matrix membranes were used for bifunctional application, physical separation and organic degradation. The membranes were subjected to pure water flux and contact angle measurements, the influence of TiO_2 were to increase the hydrophilicity of the membrane, the performance of the membrane in physical separation showed prominent results by removing oxybenzone up to 95% where as in organic degradation membrane showed 80% of degradation. The efficiency of the membrane in degradation was more prominent as compared to bare TiO_2 nanoparticles. The TiO_2 nanoparticles show around 70% of degradation, whereas, the bifunctionality of the membranes showed more prominence in removal of complete oxybenzone.

Keywords: Photocatalysis, Titanium dioxide, Oxybenzone, PSf/TiO_2 membrane

1.0 INTRODUCTION

Endocrine Disruptive Chemicals (EDCs) are natural by-products in the environment that mimic hormones in the body and can have potential impact on wildlife and humans. The endocrine system is a network of glands that release many different hormones (ductless glands that discharge hormones directly into blood stream). The major endocrine glands of the body include the pituitary, thyroid, parathyroid, adrenals, pancreas, pineal gland and gonads (ovaries in females and testes in males). Many compounds introduced into the environment by human activity (termed as EDC's) are capable of disrupting the endocrine system of animals, including fish, wildlife, and humans, affecting the immune system dysfunction, reproductive disorders, certain cancers, especially of reproductive organs, birth defects, neurological effects and low IQ.

Some of the sources of EDCs are fish, meat, industrial waste water, dairy products, cosmetics and cleaning products, pesticides, herbicides and insecticides. EDCs are natural or man-made compounds, which fit into hormone receptors, blocking the normal hormone, or acting instead of the normal hormone, in an irregular manner [1-3]

Oxybenzone, an EDC is used as a broad-band UV filter in concentrations

* Corresponding to: Mahesh Padaki (email: sp.mahesh@jainuniversity.ac.in)

of up to 10% in sunscreen products alone or in combination with other UV filters because it absorbs UVB and short-wave UVA. Beside the usage in sunscreens, Oxybenzone is incorporated in many types of cosmetic products at concentrations ranging between 0.05-0.5% for photo protection [4]. Oxybenzone is a broad range UV filter which absorbs UV light at 240 (λmax), 290 (λmax) and 325 (λmax) and since it strongly absorbs UV light, this was considered as a good choice of compound in sunscream products [5, 6] Oxybenzone when exposed to UV light was found to undergo oxidation to semiquinone intermediate which inactivates the anti-oxidant enzyme thioredoxinreductase which results in the homeostasis of the epidermis [7, 8].

In light of the above there is a lot of research going on in the area of advanced oxidation process for elimination of hazardous organic moieties. Use of semiconducting material such as TiO_2 nano particles (NPs) for the photochemical degradation of such organic pollutants is an established and known concept [9-12] and the principle behind is well understood [13-16].

Present work involves the synthesis of PSf/TiO_2 composite membranes by phase inversion process with TiO_2 NPs. PSf/TiO_2 membrane is a hybrid membrane which has semiconductor particles cause's electronic transitions from valence band to conduction band leaving behind holes in the former [17]. These electrons and holes either migrate to particle surface and become involved in redox reactions or simply liberate heat. Conduction band electrons are consumed in the reaction to reduce oxidants while holes are filled via oxidation. The conduction band electrons and valance band holes creates hydroxyl radicals or super oxide molecular oxygen which reacts with the organic compound and oxidizes the compound into non harmful products [18]. Immobilization of TiO_2 on PSf membrane significantly improves its basic applications such as water uptake and separation of contaminants [19] However since the number of nanoparticles increases the fouling mitigation effect, the membrane can be recycled many times which helps economically [20, 21] and overcome the key drawbacks of suspended process such as catalyst recovery and regeneration of spent material. The bifunctional ability of such membranes to cause both rejection of oxybenzone and its oxidation is one of the novel method.

To the best of our knowledge removal of oxybenzone were rarely found in the open literature. Known material for the removal of oxybenzone is novelty of this work. XRD and Raman spectroscopy were used to study the microstructure of the NP's and membranes, morphology of membranes and NP's were characterized by SEM, TEM and FESEM. Hydrophilicity of the membranes was investigated by contact angle and water uptake, whereas performance of the membrane in degradation as well as separation was investigated in different environmental condition. Novel approach was established in this work for removal of EDC's like oxybenzone.

2.0 METHODS

2.1 Materials

2-Hydroxy-4-methoxy-benzophenone, ammonium persulfate (AMP) (Merck brand), Polysulfone (Mw: 32000 Da) was procured from Sigma-Aldrich and titanium precursor titanium tetrachloride from Merck chemicals.

All other chemicals like 1-Methyl-2-pyrrolidone (NMP), perchloric acid, ammonia and sulpphuric acid were purchased from Merck, India and used as such.

2.2 TiO_2 NPs Preparation

The pure anatase form of TiO_2 NPs were prepared as described in [22] using 100 ml of $TiCl_4$ which was added drop wise to a liter of double distilled water and the temperature was maintained at less than 100^oC, 1 ml of concentrated H_2SO_4 was added to complete the hydrolysis followed by precipitation with NH_4OH at pH of 7-8, the precipitate was allowed to settle down and then filtered and annealed at 600^oC for 6 h to obtain TiO_2 NPs.

2.3 Preparation of PSf/TiO_2 Composite Membranes

The PSf/TiO_2 composite membranes with desired weight percent of NPs were prepared by phase inversion process. (1% NPs, 18% Polysulfone and 81% NMP). The 0.4g of NPs was taken into 16 ml of NMP of 99% purity, stirred for 5 h at room temperature and sonicated for 0.5 h for uniform dispersion. 4g of PSf (Mw= 32,000 Da), was discharged into above solution mixture and stirred for 24 h to obtain a viscous solution. Since 1% NPs and 18 % PSf with 81 % of the solvent NMP was found to ideal lower concentration of NPs, further lower concentrations of NPs were not used. The solution was casted on glass plate and dipped in coagulation bath of distilled water to get composite membrane sheet. Mixed matrix membrane was washed several times with distilled water to remove excess of solvent which might be present during the preparation process and by dipping into distilled water for 24 h and further used for photocatalytic reduction process [23]

2.4 Characterization

2.4.1 Raman Spectroscopy, UV-Visible Spectroscopy and XRD

Raman spectrum of NP's were recorded (LabRAM HR, HoribaJobinYvon, France) using 514.5 nm, air cooled Ar* laser beam with 50X objective laser intensity. UV-Visible spectra's were recorded using Schimadzu 1700 PC-UV-visible spectrophotometer. X-ray diffraction patterns of the NP's and composite membranes were recorded with Shimadzu XRD-model 7000 with Cuka radiation scan rate of 10 min^{-1} and NPs size was determined using Scheer's equation

$$D = k\lambda/\beta \cos\theta \quad (1)$$

where D is the average crystal diameter, k is a constant of 0.89, λ the radiation wavelength equal to 0.154 nm, β the full width half maximum of the diffraction peak and θ the Bragg's angle.

2.4.2 Morphological Study

SEM, TEM and a Carl Zeiss field emission Scanning electron microscope (FESEM) was used to study the morphology and microstructure of the mixed matrix membranes and NP's. The particle size and surface morphology was determined using Scanning electron microscope and a high resolution transmission electron microscope (Technai 10 Phillips).

2.4.3 Water Uptake and Contact Angle Measurements

Water uptake of the prepared membrane was performed by weight change during its soak in distilled water. Membranes were thoroughly rinsed with distilled water, and then dried in vacuum desiccators with a vacuum of 120 mm Hg for 24 h. The dried membrane was made in 1 cm^2 small pieces and later immersed in distilled water. The membranes were taken out after 24 h interval of time, and excess water on the surface was gently removed by a blotter, then the weight of the soaked membranes was quickly measured. Water uptake percentage was calculated using the following formula.

$$\%Uptake = \left(\frac{w_w - w_d}{w_d} \right) \times 100 \qquad (2)$$

where W_w and W_d are the weights of wet and dried membranes respectively. The contact angle between the water and the membrane was measured by using FTA-200 Dynamic contact angle measurement by sessile drop method. A water droplet was placed on the membrane at five different places; the average of five is reported.

2.5 Membrane Performance Study

2.5.1 Photocatalytic Oxidation

Photocatalytic experiment was conducted in self-constructed UV hood. UV source of 125 W Phillips mercury vapor lamp whose wavelength peaked around 350-400 nm, with a photon flux of 77.5 W/m^2 was used for UV irradiations. The experiments were carried out by self-designed procedure. The experimental design was submitted in supplementary data. A round membrane sheet of 180 cm^2 was directly exposed to light along with the 250 ml of oxybenzone solution of 3 ppm taken in a reactor vessel and carried out using, control, TiO_2 NPs, PSf membrane and TiO_2/PSf membrane. The complete study was performed to evaluate catalytic capacity of TiO_2 NPs, hybrid membranes and impact of AMP on catalytic activity. The concentration of the oxybenzone was determined by UV-Visible spectrophotometer (Shimadzu 1800PC) with max= 235 nm wavelength. 10 mL of the treated samples were collected for every 15 min and concentration was determined. C/C_0 was calculated using concentration of feed and treated sample (C = concentration of treated sample; C_0 = concentration of feed) at different intervals of time. Further to validate the degradation of oxybenzone was analyzed using GC-MS. Shimadzu GCMS-QP2010 ultra instrument which has columns DB-FFAP (30x0.32 mm ID: 1.8 um) were used with the injector port, temperature was maintained at 2500C, 1 µL was the injection volume and Helium was used as a carrier gas, ion source temperature and interface temperature was maintained at 2000^{o}C and 2300^{o}C, respectively..

2.5.2 Rejection of Oxybenzone

The rejection of oxybenzone was carried by using dead end self-constructed filtration unit. The experimental set up was followed as described in Jyothi *et al.* [24]. Prepared membrane was cut into round shape of 5 cm2 and fixed at the bottom of the unit and filled with 500 ml of 10 ppm oxybenzone solution. Nearly 20 mL of solution was collected at different applied pressures and analyzed for concentration of oxybenzone at λmax=235 nm using UV-Visible spectrophotometer [25] The percent rejection was calculated by the below equation

$$\%\, Rejection = \left(1 - \frac{Cp}{Cf}\right) \text{x}100 \qquad (3)$$

where C_p and C_f are permeate and feed concentrations respectively.

3.0 RESULTS AND DISCUSSION

3.1 Characterization of NPs and Membranes

3.1.1 XRD and Raman Studies

Figure 1 shows the XRD patterns of TiO2 NPs (a), PSf membrane (b) and PSf/TiO2 mixed matrix membrane (c). X-ray patterns for the prepared photocatalyst reveal a sharp peak at 2θ = 25.3oindicating an anatase phase and since there is no peak observed at around 2θ = 27o which is characteristic peak of rutile TiO2 (JCPDS no.: 88-1175). It was confirmed that the NPs obtained is complete anatase, the spectrum matches with standard, average diameter of NPs was found to be 17 nm as calculated from Scherrer's equation. XRD patterns of hybrid membranes evidenced the incorporation of the photocatalyst into the polymer matrix and d-spacing was found to be 3.49 Å. There was a complete retention of anatase phase in TiO_2/PSf membrane. The crystallite size of the NPs in the membrane was significantly lesser than the bare TiO_2 NPs. This is because of the higher radius of gyration of the polymer (than the NPs), exerting a strain on the crystallites, thus affecting the size and crystallite dispersion on the membrane surface [26].

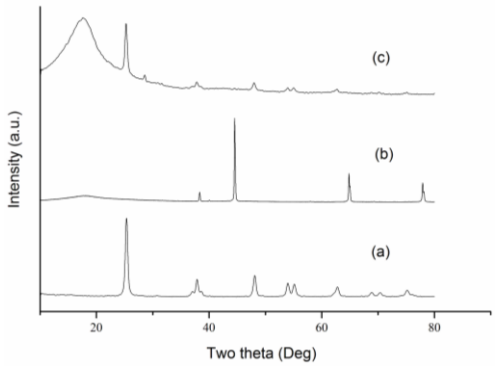

Figure 1 XRD Pattern of a) TiO_2 NPs b) PSf membrane c) TiO_2/PSf membrane

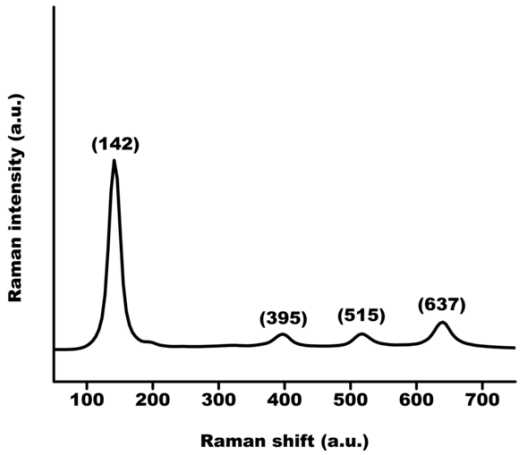

Figure 2 Raman Spectra of TiO2 NPs

Figure 2 depicts the Raman spectrum for anatase TiO_2 the following allowed bands at 142 cm^{-1} (Eg), 395 cm−1 (B1g), 515 cm^{-1} (A1g), and 637 cm^{-1} (Eg), and the peaks obtained are in agreement with the XRD data, substantiating the presence of the crystalline anatase phase.

3.1.2 Surface Morphology

Figure 3a and 3b shows the SEM and TEM images of TiO2 NP's. The agglomerated particles were observed in Scanning electron microscope and a high resolution transmission electron microscope (Phillips 10) shows uniform size of the particles. SEM images are taken on a scale of 10µm and TEM images were taken on a scale

of 100 nm. In TEM image it can clearly observed that white dots on particles which shows porous in nature. The particle size was found to be around 20 nm. However, Figure 4a and 4b depicts surface image of the PSf and PSf/TiO_2 membrane respectively. In Figure 4b the distributed NPs spherical agglomerates (inset) on surface layer of polymer were observed. Both the membranes were unstable in higher energy electron bombardment, hence, canal like structure were observed and indicated breakage of membranes by high electron bombardment.

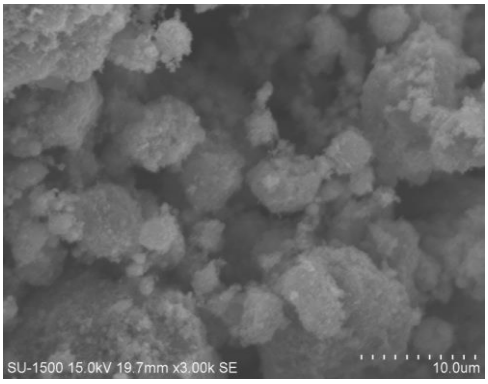

Figure 3a SEM image of TiO_2 NPs

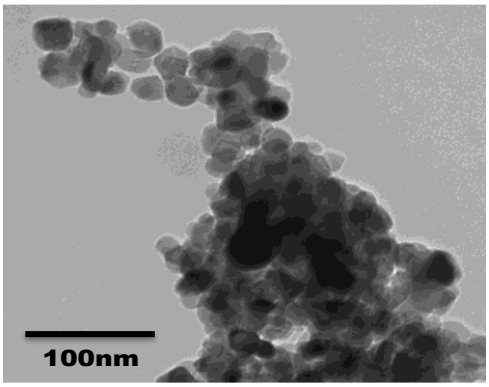

Figure 3b TEM image of n-TiO_2 NPs

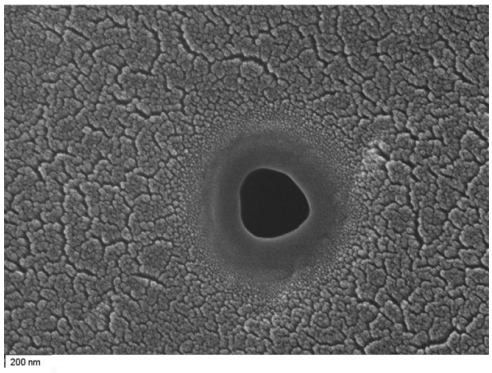

Figure 4a FESEM image of PSf membrane

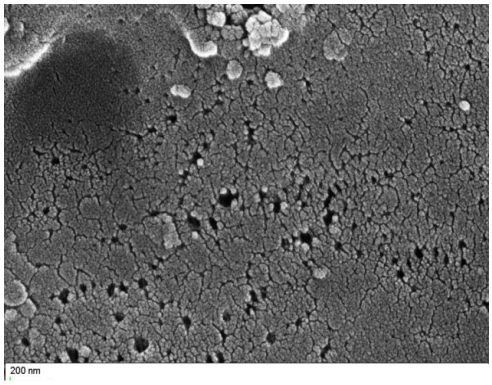

Figure 4b FESEM image of PSf/TiO_2 membrane

3.2 Wetability Study of Membranes

The water uptake and contact angle are the main two parameters to determine the hydrophilicity of the membrane [27]. Figure 5 depicts the contact angle and water uptake for the prepared composite membrane. The contact angle of plane PSf decreases from 76 ±2 0 to 72 ± 20 and the water uptake had increased from 17 to 62.2 %, by the incorporation of TiO_2 NPs. which are semi conducting metal oxides of hydrophilic in nature [28], which has more hydroxyl polarity and is able to interact with water molecules through Van der Waal's force and hydrogen bonding, which helps to enhance the hydrophilicity of the membrane [29]. However, It is also possible that the higher affinity of TiO_2 for water

compared to polysulfone increases the penetration velocity of water into mixed matrix membrane during the phase inversion process [30]. This causes porous structure on membrane surface. Hence, PSf/TiO_2 membrane is hydrophilic as well as porous in nature.

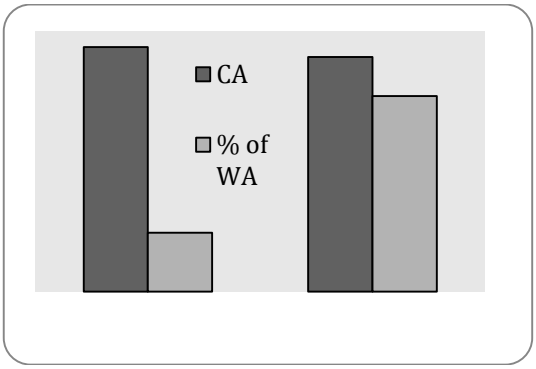

Figure 5 Water uptake and contact angle of plane PSf and PSf/TiO_2 composite membranes

3.2.1 Rejection of Oxybenzone using PSf/TiO_2 Composite Membrane

The rejection of oxybenzone was carried out in dead filtration unit at different pressure ranging from 200 k Pa to 1000 k Pa. Figure 6 shows the extent of rejection and flux with respect to applied pressure. The experiment was carried out using both neat PSf and PSf/TiO_2 composite membrane. Since neat PSf is hydrophobic in nature, there was no flux and rejection observed at different pressures, but with hybrid membranes, flux was observed at lower pressures as shown in Figure 6. The rejection of oxybenzone was 95.48 %, with 3.97 L/m^2h flux at 200 k Pa. As discussed earlier TiO_2 enhances the porous nature and hydrophilicity. Membrane showed better interaction with water as compared to oxybenzone, because of hydrophilic TiO_2 NPs. The rejection percent was decreased to 77.6% and flux was increased to 22.01 L/m^2h with increase in pressure to 1000 k Pa. It emits that in higher pressure the membrane porous are enlarging. Hence rejection was decreased in higher pressure.

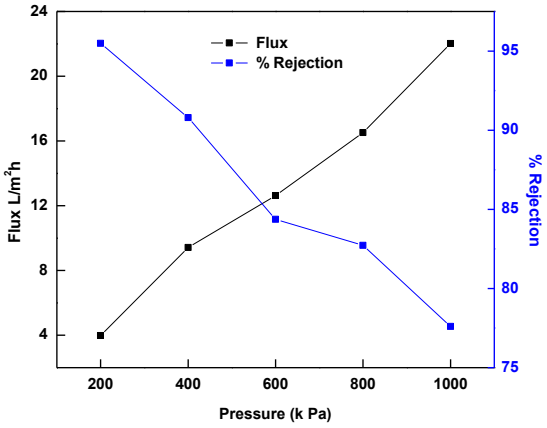

Figure 6 Plot of pressure versus flux and % rejection for PSf/TiO_2 composite membrane

3.2.2 Photocatalytic Oxidation of Oxybenzone

Figure 7a-c represents the photooxidation in different experimental conditions. It depicts the importance of (i) light, (ii) nature of light (ii) TiO_2 NPs, (iii) immobilized TiO_2 and (iv) AMP for the oxidation. It is clear from the graph that the TiO_2 NPs enhances the photo oxidation in presence of AMP. An enhancement of oxidation was observed on immobilization of TiO_2 (supported on a membrane).

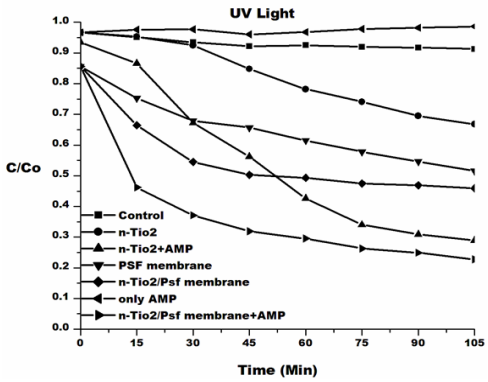

Figure 7a Concentration of oxybenzone at the end of 105 min under normal light

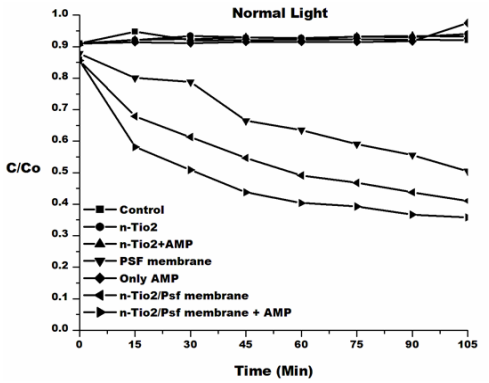

Figure 7b Concentration of oxybenzone at the end of 105 min under normal light

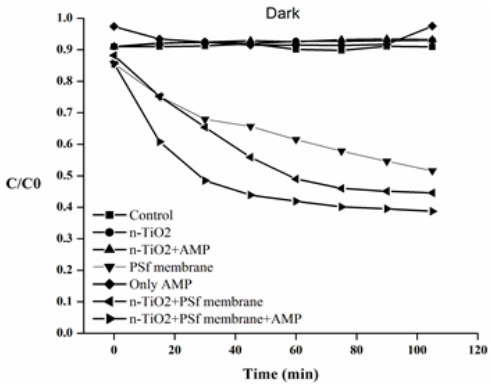

Figure 7c Concentration of oxybenzone at the end of 105 min under Dark condition

From the several experiment the following results are summarized. The plane membrane doesn't have the property to oxidize EDC, TiO_2 NPs deposited on top of the membrane are responsible for oxidizing the EDC, similarly light alone doesn't causes the degradation of oxybenzone from the Figure 7a and Figure 7b it depicts that there is no degradation observed only when UV and normal light was used, similarly Figure 7b and Figure 7c shows that use of TiO_2 NPs and AMP under normal light and dark has negligible effect on oxidation. Lone AMP under UV irradiation doesn't have any effect on photolysis of EDC (Figure 7a). From Figure 7a it was clear that around 80% of the oxybenzone can be degraded using TiO_2/PSf membrane with AMP. It has been well known that $S_2O_8^{2-}$is decomposed to $SO^{4-\bullet}$ radical under UV irradiation which is a strong oxidant. $SO^{4-\bullet}$ radical oxidizes the EDC molecule, leading to partial degradation. However around 80% of the oxidation occurs in presence of UV light, AMP and membrane. With bare NPs, a small decrease of about 30% was observed. The photocatalyst with a band gap of 3.1 eV responds well to the UV light to produce the electron-hole pair and cause redox reactions thereof. However, the produced electrons and holes remain insufficient to cause complete reduction. The percent of recombination of electrons and +ve holes affects photocatalytic efficiency in a big way. While considering a NP's the concept of deep traps and defects may not be applicable. The defects or the irregularities are only with the surface states and the polymer matrix for TiO_2 allows easy induction of electrons thus maximizing the charge separation time and act as carrier traps, avoiding recombination which later detraps the same to the NPs surface leading to a good interfacial charge transfer [31]. Thus, the importance of polymer matrix on to which the TiO_2 NPs has been incorporated, contributes to charge carrier separation and effectively causes redox reactions. The positive holes that cause oxidative reactions have very strong oxidizing power and they can directly oxidize EDC. The photo generated electron hole pairs on internal recombination, reduces the effectiveness of TiO_2 photocatalyst. AMP serves as electron acceptor and traps the conduction band electron before recombination [32] Thus, superoxide radical (or on cyclic reaction under acidic conditions can give hydroperoxyl or hydroxyl radicals) which cleaves the organic oxybenzone moiety. The electron acceptors are known to generate

hydroxyl radicals, which are thought to be primary oxidizing species. They are known to react very rapidly with organic moiety to yield hydroxylated radicals and subsequent reaction of these adduct radicals can lead to mineralization of polynuclear hydrocarbons [33]. The ability of a semiconductor to undergo photo induced electron transfer to adsorbed species on its surface is governed by band energy positions of the semiconductor and the redox potentials of the adsorbate. The relevant potential level of the acceptor species is thermodynamically required to be below (more positive than) the conduction band potential of the semiconductor. The potential level of the donor needs to be above (more negative than) the valence band position of the semiconductor in order to donate an electron to the vacant hole. AMP influences the band edge positions of semiconductor, surface charge of TiO_2 NPs. Thus, the efficiency of the reaction increases. SO_4^{2-} radicals can further give $SO^{4-\bullet}$ thus producing more hydroxyl radicals.

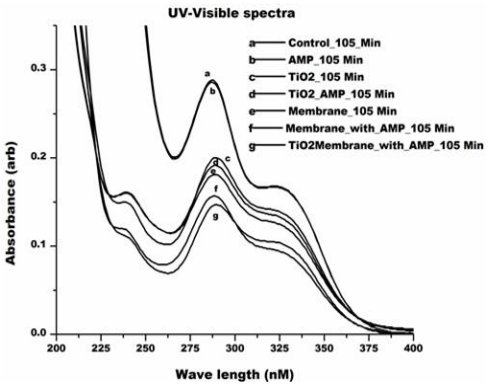

Figure 8 UV-Visible spectra of oxybenzone at the end of 105 min under UV light

Figure 8 shows UV-Visible spectra of oxybenzone at the end of 105 min under UV light. In the figure, (a) represents the spectra of original compound before any irradiation. It shows prominent peaks at 290nm and 325nm. The peak at 290nm is clearly the B-band of an extended Ketone. It is important to specify that this peak at 290 nm appears more prominently with degradation which could also be explained as a secondary band of benzoic acid, formed as an intermediate. The high conjugation present in the molecule gives a peak at 325nm, which is also the □max of the EDC molecule. Curve (b) indicates the system where only AMP is used for degradation, negligible change in spectra is observed even after 105 minutes of illumination. Curve (c) indicates the system where lone TiO_2 NPs were used; it was evident from the spectra that there is some amount of degradation of EDC. Curve (d) to curve (f) indicates the gradual decrease in the intensities of the peaks with the use of membrane and AMP and curve (g) where TiO_2/PSf membrane with AMP is used, shows the maximum decrease in the intensities of the peaks indicating around 80% of the degradation of EDC.

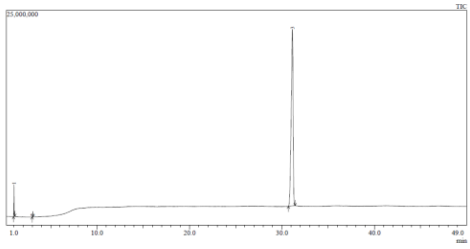

Figure 9a GC-MS chromatogram of standard oxybenzone

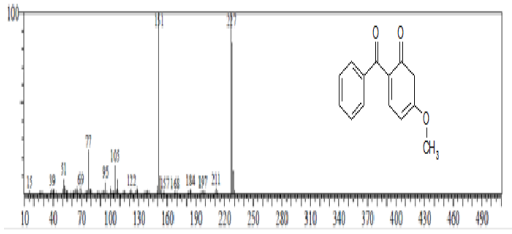

Figure 9b MS Chromatogram of standard oxybenzone (keto form)

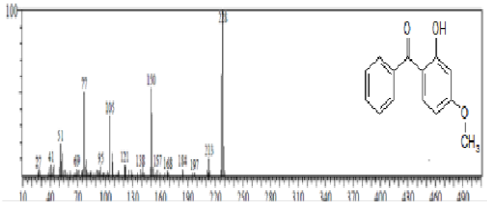

Figure 9c MS Chromatogram of standard oxybenzone (enol form)

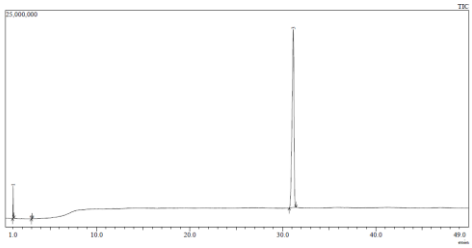

Figure 10a GC-MS chromatogram of oxybenzone after 1-h photodegradation

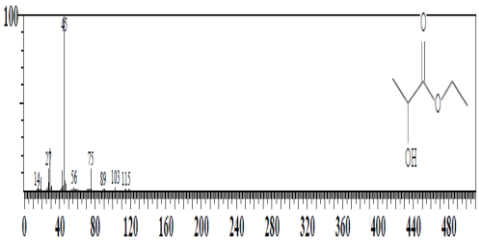

Figure 10b MS Chromatogram of an open chain intermediate

It was clear from the GC-MS spectra that the oxybenzone had been successfully degraded using nano particle TiO_2 and AMP (Figure 9a and Figure 10a)

Figure 9a depicts the GCMS chromatogram of standard oxybenzone, which shows a strong peak at a retention time of 31 min with a peak area of 97.70% and peak height of 84.40% and also Figure 9b and Figure 9c shows the keto-enol forms of the oxybenzone peaks at 227(M+) and 228(M+) respectively [34]. Figure 10a depicts the GC-MS analysis of the UV irradiated mixture taken after 1h, and it showed the degradation of oxybenzone i.e. at a retention time of 31 min the peak area was found to be 1.1% with a peak height of 0.62% suggesting the degradation of oxybenzone. Also there were several open chain intermediates formed during the course of the reaction. Figure 10b depicts one of the open chain intermediate formed.

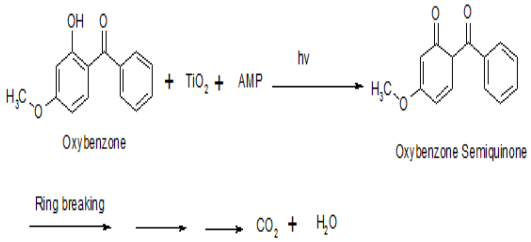

Figure 11 Schematic representation of photocatalysis

The products were identified based on their molecular ion and mass spectrometric fragmentation peaks. The point of cleavage on irradiation is found to be =C-C=O in the fused benzene ring by addition of OH radicals to get the semiquinone as shown in Figure 11. Further degradation of the semiquinone aromatic rings takes place to form open chain compounds and finally to form carbon dioxide and water. It was also observed from the UV spectral data that the strong absorbance peak of oxybenzone at 235 nM (λmax) had decreased substantially after exposure to UV light, and similarly when the samples were analyzed from GC-MS the peak corresponding to oxybenzone had almost disappeared indicating the successful degradation of the oxybenzone using TiO_2 NPs in presence of AMP under UV light (Figure 9a and Figure 10a)

4.0 CONCLUSION

Polysulfone and titanium dioxide mixed matrix membrane and bare TiO_2 NPs were used for removal of

oxybenzone. The separation was achieved in both the process: Photocatalytic degradation and physical separation, thus about 96 % of oxybenzone was removed by physical separation at a pressure of 200 kPa whereas 80% of Oxybenzone was degraded by photocatalytic process. In the case of photolysis, several intermediates were formed and unable complete removal of chemicals from water, where as in filtration process maximum rejection was observed without any intermediates. Hence, in this case membrane filtration methodology is better than photocatalytic process.

REFERENCES

[1] Johnson. A. C., Sumpter. J. P. 2001. Removal Of Endocrine-Disrupting Chemicals In Activated Sludge Treatment Works. *Environmental Science and Technology*. 35 (24): 4697–4703.

[2] Schlumpf, M. B. Cotton. M. C. Haller. V. Steinmann. B. Lichtensteiger. W. 2001. In Vitro And In Vivo Estrogenicity Of UV Screens. *Environmental Health Perspectives.* 109(3): 239–244.

[3] Kasichayanula, S. House. J. D. Wang. T. Gu. X. 2007. Percutaneous Characterization Of The Insect Repellent DEET And The Sunscreen Oxybenzone From Topical Skin Application. *Toxicology and Applied Pharmacology.* 223(2): 187–194.

[4] Burnett, M. E. Wang. S. Q. 2011. Current Sunscreen Controversies: A Critical Review. *Photodermatology, Photoimmunology & Photomedicine.* 27(2): 58–67.

[5] Shaach, N. A. Griffin, P. M. Andemichael. G. 1990. Interpretation And Evaluation: Spectroscopic Data Of Sunscreens. *Sunscreens (Cosmetics).* 37–541

[6] Runger, T. M. Lehman, P. Matthies. C. Schauder. S. Munzberger. C. 1995. Recommendation Of A Photo Patch Test Standard Series By The German-Language Working Group. *Photopatch-Test, Hautarzt.* 46: 240–243.

[7] Sundaram, C., Koster, W., Schallreuter, K. U. 1990. The Effect Of UV Radiation And Sun Blockers On Free Radical Defence In Human And Guinea Pig Epidermis. *Anti Dermatol Res*. 282: 326–331.

[8] Nick, Serpone, Daniele Dondi. Angelo. Albini. 2007. Inorganic And Organic UV Filters: Their Role And Efficacy In Sunscreens And Suncare Products. *Inorganica Chimica Acta*. 360: 794–802.

[9] Khodja, A. A. Sehili. T. Pilichowski, J. F. Boule. P. 2001. Photocatalytic Degradation of 2-phenylphenol on TiO2 and ZnO in Aqueous Suspensions. *J. Photochem. Photobiol. A: Chem*. 141: 231–239.

[10] Chen, D., Ray, A. K. 1998. Photodegradation Kinetics Of 4-nitrophenol In TiO2 Suspension. *Water Res.* 32: 3223–3234.

[11] Gomes da Silva, C. Faria, J. L. 2003. Photochemical And Photocatalytic Degradation Of An Azo Dye In Aqueous Solution By UV Irradiation. *J. Photochem. Photobiol. A: Chem*. 155: 133–143.

[12] Kusvuran, E., Gulnaz, O., Irmak. S., Atanur, O. M., Yavuz, H. I., Erbatur, O. 2004. Comparison Of Several Advanced Oxidation

Process For The Decolorization Of Reactive Red 120 Azo Dye In Aqueous Solution. *J. Hazardous Mater.* 109: 85–93

[13] Fox, M. A., Dulay, M. T. 1993. Heterogeneous Photocatalysis. *Chem. Rev.* 93: 341–357.

[14] Galindo, C., Jacques, P., Kalt, A. 2000. Photochemical And Photocatalytic Degradation Of An Indigoid Dye: A Case Study Of Acid Blue 74 (AB74). *J. Photochem. Photobiol. A: Chem.* 141: 47–56.

[15] Turchi, C. S., Ollis, D. F. 1990. Photocatalytic Degradation Of Organic Water Contaminants: Mechanism Involving Hydroxyl Radical Attack. *J. Catal.* 122: 178–192.

[16] Irmak, S., Kusvuran, E., Erbatur. O. 2004. Degradation Of 4-chloro-2-methylphenol In Aqueous Solution By UV Irradiation In The Presence Of Titanium Dioxide. *Appl. Catal. B: Environ*. 54: 85–91.

[17] Yang, Y., Zhang, H., Wang, P., Zheng, Q., Li, J. 2007. The Influence Of Nano-Sized TiO2 Fillers On The Morphologies And Properties Of PSFUF Membrane. *J. Membr Sci*. 288: 231–238.

[18] Davide Vionea, Claudio Mineroa, Valter Maurinoa, M. Eugenia Carlottib, Tatiana Picatonottoa, Ezio Pelizzettia. 2005. Degradation Of Phenol And Benzoic Acid In The Presence Of A TiO2-based Heterogeneous Photocatalyst. *Applied Catalysis B: Environmental.* 58: 79–88.

[19] Gonu, Kim, Wonyong, Choi. 2010. Charge-Transfer Surface Complex Of EDTA-TiO2 And Its Effect On Photocatalysis Under Visible Light. *Appl. Catal. B.* 100: 77–83.

[20] Seree, Tuprakay, Winai, Liengcharensit. 2005. Lifetime And Regeneration Of Immobilized Titania For Photocatalytic Removal Of Aqueous Hexavalent Chromium. *Journal of Hazardous Materials.* 124: 53–58.

[21] Yang, Y., Wang, P. 2006. Preparation And Characterizations Of A New PS/TiO2 Hybrid Membrane By Sol-Gel Process. *Polymer*. 47: 5671–5681.

[22] Swetha, S., Singh, M. K., Minchitha, K. U., Balakrishna, R. G. 2012. Elucidation of Cell Killing Mechanism by Comparative Analysis of Photoreactions on Different Types of Bacteria. *Journal of Photochemistry and Photobiology*. 88: 414–422.

[23] Teow, Y. H., A. L. Ahmaqd, J. K. Lim, B. S. Ooi. 2012. Preparation And Characterization Of PVDF/TiO2 Mixed Matrix Membrane Via In Situ Colloidal Precipitation Method. *Desalination*. 295: 61–69.

[24] Jyothi, M. S., Vignesh Nayak, Mahesh Padaki, R. Geetha Balakrishna, A. F. Ismail. 2014. The Effect Of UV Irradiation On PSf/TiO2 Mixed Matrix Membrane For Chromium Rejection. *Desalination.* 354: 189–199.

[25] Mahesh, Padaki, Arun, M. Isloor, Ganesh, Belawadi, Narayan, Prabhu. K. 2011. Preparation and Performance Study of Poly(Isobutylene-alt-maleic anhydride) [PIAM] and Polysulfone [PSf] Composite Membranes Before And After Alkali Treatment. *Ind. Eng. Chem. Res*. 6528–6534.

[26] Yoshitake Masuda. 2011. Nanofabrication edited by. ISBN 978-953-307-912-7.

[27] Mahesh, Padaki, Arun, M. Isloor. Pikul, Wanichapichart, Ahmad, Fauzi, Ismail. 2012. Preparation And Characterization Of Sulfonated Polysulfone And N-phthloyl Chitosan Blend Composite Cation Exchange Membrane For Desalination. *Desalination*. 298: 42–48.

[28] Liu, P., Lin, H. X., Fu, X. Z. 1995. Preparation Of The Doped Tio_2 Film Photocatalyst And Its Bactericidal Mechanism. *Chin J Catal.* 20(3): 327–328.

[29] Sakai, N. Fukuda, K. Shibata, T. Ebina, Y. Takada, K. Sasaki, T. 2006. Photoinduced Hydrophilic Conversion Properties Of Titania Nanosheets. *J. Phys. Chem. B*. 110: 6198–6203.

[30] Rahimpour, A., S. S. Madaemi, A. H. Taheri, Y. Mansourpanah. 2008. Coupling TiO_2 Nanoparticles With UV Irradiation For Modification Of Polyethersulfone Ultrafiltration Membranes. *J. Membr. Sci.* 313: 158.

[31] Bae, T. H., T. M. Tak. 2005. Effect of TiO2 Nanoparticles On Fouling Mitigation Of Ultra-Filtration Membranes For Activated Sludge Filtration. *J. Membr. Sci.* 240: 1–8.

[32] Shifu, C. and L. Yunzhang. 2007. Study On The Photocatalytic Degradation Of Glyphosate By Tio_2 Photocatalyst. *Chemosphere*. 67(5): 1010–1017.

[33] Bahnemann, W., M. Muneer, and M. M. Haque. 2007. Titanium Dioxide-Mediated Photocatalysed Degradation Of Few Selected Organic Pollutants In Aqueous Suspensions. *Catalysis Today*. 124(3-4): 133–148.

[34] Kazuo Ikeda, Sukeji Suzuki, Yohya Watanabe. 1990. Determination Of Sunscreen Agents In Cosmetic Products By Gas Chromatography And Gas Chromatography-Mass Spectrometry. *Journal of Chromatography A*. 513: 321–326.